Nanoscale

Accepted Manuscript

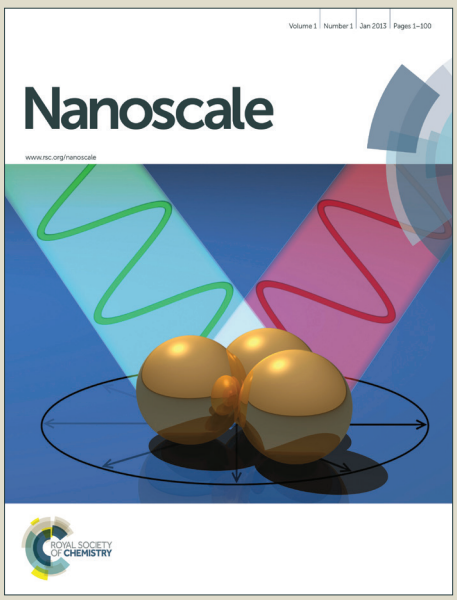

This is an *Accepted Manuscript*, which has been through the Royal Society of Chemistry peer review process and has been accepted for publication.

Accepted Manuscripts are published online shortly after acceptance, before technical editing, formatting and proof reading. Using this free service, authors can make their results available to the community, in citable form, before we publish the edited article. We will replace this *Accepted Manuscript* with the edited and formatted *Advance Article* as soon as it is available.

You can find more information about *Accepted Manuscripts* in the Information for Authors.

Please note that technical editing may introduce minor changes to the text and/or graphics, which may alter content. The journal's standard Terms & Conditions and the Ethical guidelines still apply. In no event shall the Royal Society of Chemistry be held responsible for any errors or omissions in this *Accepted Manuscript* or any consequences arising from the use of any information it contains.

ROYAL SOCIETY OF CHEMISTRY

www.rsc.org/nanoscale

Dynamic Article Links ►

Cite this: DOI: 10.1039/c0xx00000x

www.rsc.org/xxxxxx

Paper

Facile synthesis of zwitterionic polymer coated core–shell magnetic nanoparticles for highly specific capture of N-linked glycopeptides

Yajing Chen,[‡a] Zhichao Xiong,[‡a] Lingyi Zhang,[a] Jiaying Zhao,[a] Quanqing Zhang,[b] Li Peng,[a] Weibing Zhang,[*ab] Mingliang Ye,[b] and Hanfa Zou[*b]

Received (in XXX, XXX) Xth XXXXXXXXX 20XX, Accepted Xth XXXXXXXXX 20XX
DOI: 10.1039/b000000x

The highly selective and efficient capture of glycosylated proteins and peptides from complex biological samples is of profound significance to the discovery of disease biomarkers in biological systems. Recently, hydrophilic interaction liquid chromatography (HILIC)-based functional materials have been extensively utilized for glycopeptide enrichment. However, the low amount of immobilized hydrophilic groups on the affinity material has limited the specificity, detection sensitivity and binding capacity in the capture of glycopeptides. Herein, a novel affinity material was synthesized to improve the binding capacity and detection sensitivity for glycopeptides by coating poly (2-(methacryloyloxy) ethyl) dimethyl-(3-sul-fopropyl) ammonium hydroxide (PMSA) shell onto Fe_3O_4@SiO_2 nanoparticles, taking advantage of reflux–precipitation polymerization for the first time (denoted as Fe_3O_4@SiO_2@PMSA). The thick polymer shell endows the nanoparticles with excellent hydrophilic property and a great deal of functional groups on the polymerization chains. The resulting Fe_3O_4@SiO_2@PMSA demonstrated an outstanding ability for glycopeptides enrichment with high selectivity, extremely high detection sensitivity (0.1 fmol), large binding capacity (100 mg g^{-1}), high enrichment recovery (above 73.6 %) and rapid magnetic separation. Furthermore, in the analysis of real complicated biological sample, 905 unique N-glycosylation sites from 458 N-glycosylated proteins were reliably identified in three replicate analysis of 65 μg protein sample extracted from mouse liver, showing the great potential in detection and identification of low-abundant N-linked glycopeptides in biological samples.

Introduction

Protein glycosylation, one of the most significant post-translational modifications (PTMs) in proteome, attaches great importance to multiple biological processes including signal transduction, intracellular transport, immune response and cell growth.[1-4] Abnormal glycosylation is associated with various diseases such as cancer and neurodegenerative diseases.[5] To better understand these biological processes as well as discover disease biomarkers, it is necessary to identify glycoproteins and determine their glycosylation sites. Currently, mass spectrometry (MS)-based techniques have become the most important and effective tools for analyzing and characterizing protein glycosylation. Unfortunately, the tremendous heterogeneity of each glycosylation site, inherent low abundance of glycopeptides and serious signal suppression caused by the co-existence of abundant non-glycosylated peptides make the direct MS analysis of glycopeptides still a challenge. Therefore, an efficient approach for glycopeptide enrichment from complex biological sample prior to MS analysis is imperative.

Up to now, several materials and methods embracing lectin affinity chromatography,[6-8] boronic acid affinity chromatography,[9-13] hydrazide beads,[14, 15] titanium dioxide,[16] and hydrophilic interaction chromatography (HILIC) adsorbents[17, 18] have been developed for glycopeptides enrichment. Among them, the enrichment strategy based on HILIC has been well developed and gained increasing popularity due to its simple operating process, high selectivity, excellent reproducibility, no bias and reversible alterations of glycan composition. A variety of hydrophilic matrices, such as sepharose, cellulose, saccharides, ZIC-HILIC beads and metal-organic framework, [19-22] have been used for the selective separation and extraction of glycopeptides. Nevertheless, the relatively low density of the hydrophilic molecules on the surface of traditional HILIC absorbents has limited the specificity, detection sensitivity and binding capacity of glycopeptides. It was demonstrated that HILIC beads with a high amount of functional molecules bonded could further improve the enrichment performance. [23] Thus, it is highly desirable for novel HILIC materials with abundant hydrophilic groups to improve the glycopeptides enrichment efficiency.

In the last decade, magnetic nanoparticles have gained immense interest due to their unique biocompatibility, easy preparation, versatile modification and rapid magnetic response, and are widely used in magnetic resonance imaging, drug delivery, sensing, and proteomic research. [24-28] A combination of magnetic nanomaterial and covalently bonded hydrophilic functional molecule could simultaneously achieve the simple and efficient capture of the glycopeptides from the complex mixture

Nanoscale Accepted Manuscript

by magnetic separation. Several kinds of functionalized magnetic nanoparticles (e.g. poly (4-vinyl-pyridinium ethanesulfonate) coated Fe_3O_4,[29] Fe_3O_4@SiO_2@PEG-Maltose[23]) were developed and showed great selectivity for glycopeptides. Yet, the synthesis procedures of these materials were tedious. Recently, Zou et al.[30] fabricated a kind of multilayer polysaccharide shells coated magnetic nanoparticles using a simple and convenient approach (layer-by-layer) and the obtained composite material exhibited high selectivity, high detection sensitivity and large binding capacity for glycopeptides enrichment. Fang et al. [31] developed an one-pot method for the synthesis of chitosan coated magnetic nanoparticles, and the thick chitosan shell was beneficial to improve the enrichment efficiency. Notwithstanding these successful examples, the design and synthesis of novel hydrophilic polymer coated magnetic nanoparticles is drawing extensive attentions to the improvement of the detection sensitivity and binding capacity of glycopeptides.

Zwitterionic molecules functionalized materials are well-known superhydrophilic and ultralow biofouling materials. [32] The zwitterionic groups on the nanoparticles can bind water molecules more strongly via electrostatically induced hydration, in comparison with the water retention materials based on hydrogen-bonding-induced hydration. The large amount of the zwitterionic groups enables a thick layer of water molecules, which contributes greatly to the stronger hydrophilic interaction.[33-36] Among silica based HILIC materials, ZIC-HILIC has shown the best enrichment performance in the analysis of protein glycosylation. [37, 38] However, ZIC-HILIC materials related magnetic nanoparticle have rarely been reported. Yeh et al. [29] prepared zwitterionic polymer coated magnetic nanoparticles by employing spontaneous acid-catalyzed polymerization. Being applied for the glycopeptides enrichment, the material presented high selectivity and recovery. However，the synthesis process was tedious, and the thickness of polymer shell was difficult to control and lack of stability. Therefore, the synthesis of zwitterionic polymer coated magnetic nanoparticles by a convenient, effective and robust method for glycopeptides enrichment would be very attractive.

Herein, we report a facile approach for the synthesis of zwitterionic polymer coated magnetic nanoparticle (Fe_3O_4@SiO_2@PMSA) via reflux–precipitation polymerization for the first time. The thick zwitterionic polymer shell endows the composite not only with excellent hydrophilic surface property, but also with a great deal of zwitterionic functional sites on the polymerization chains for high detection sensitivity and large binding capacity of glycopeptides. Moreover, the unique magnetic property will facilitate the rapid and complete recovery of the composite. The specificity, detection sensitivity, enrichment capacity and enrichment recovery of Fe_3O_4@SiO_2@PMSA for glycopeptides enrichment have been evaluated by using different biological samples. Besides, the practical applicability of Fe_3O_4@SiO_2@PMSA was demonstrated by capture of low-abundance of glycopeptides in tryptic digest of proteins extracted from mouse liver. The outstanding selectivity, extreme sensitivity, excellent enrichment recovery of glycopeptides, and high magnetic susceptibility also revealed its great capability in glycoproteome analysis for real biological samples.

Experimental section

Materials and chemicals

Iron (III) hexahydrate ($FeCl_3 \cdot 6H_2O$), ethanol, ethylene glycol (EG), ammonium hydroxide ($NH_3 \cdot H_2O$, 28 wt%), tetraethyl orthosilicate (TEOS) and sodium acetate (NaAc) were obtained from Tianjin Chemical Plant (Tianjin, China). γ- methacryloxypropyltrimethoxysilane (MPS), 3-methacryloxypropyltrimethoxysilane, N, N'-methylenebisacrylamide (MBA), methacrylic acid (MAA), trifluoroacetic acid (TFA), HPLC grade acetonitrile (ACN) and ammonium bicarbonate (NH_4HCO_3) were purchased from Aladdin (Shanghai, China). 2,2-Dimethoxy-2-phenylacetophenone (DMPA) was from Acros Organics (New Jersey, USA). PNGase F was from New England Biolabs (Ipswich, MA). Human serum immunoglobulin G (human IgG), chicken avidin, horseradish peroxidase (HRP), trypsin (TPCK treated), dithiothreitol (DTT), iodoacetamide (IAA) and 2, 5-dihydroxyl benzoic acid (DHB) were got from Sigma-Aldrich (St, Louis, MO, USA). 2, 2-azobisisobutyronitrile (AIBN) was supplied by Sinopharm Chemical Reagents Company (Shanghai, China), GELoader tips (20 μL) were purchased from Eppendorf (Hamburg, Germany). All the chemical agents were used without further purification. Purified water was obtained with a Milli-Q apparatus (Millipore, Bedford, MA, USA).

Synthesis of Fe_3O_4@SiO_2@PMSA nanoparticles

The Fe_3O_4 nanoparticles were firstly prepared by means of a solvothermal reaction, and then coated with a thin layer of SiO_2 through a sol-gel process, subsequently modified with γ-MPS to obtained Fe_3O_4@SiO_2-MPS.[39-41] The procedure was described in detail in ESI †. The coating of PMSA layer onto Fe_3O_4@SiO_2-MPS nanoparticles was carried out by a one-step reflux-precipitation polymerization of MSA in mixed solvent of acetonitrile and water, with MAA as the auxiliary monomer, MBA as the cross-linker and AIBN as the initiator. Typically, 50 mg of the as prepared Fe_3O_4@SiO_2-MPS nanoparticles were dispersed ultrasonically in 80 mL of acetonitrile/water (3:1, v/v) in a dried 100 mL single-necked flask. Then, 200 mg of MSA, 50 μL of MAA, 200 mg of MBA and 6 mg of AIBN were added together into the flask. With ultrasonication for 20 min, the flask was submerged in a heating oil bath. The reaction mixture was then heated from ambient temperature to 95 ℃within 30 min and reacted for 1.5 h under the micro-boiling state. The obtained Fe_3O_4@SiO_2@PMSA nanoparticles were collected by magnetic separation and washed with ethanol for 3 times to eliminate the excessive reactants and the self-polymerized PMSA. Finally, the product was dried under vacuum at 50 ℃ for 24 h.

Synthesis of monolayer MSA molecules functionalized nanoparticles (Fe_3O_4@SiO_2-MSA)

Fe_3O_4@SiO_2-SH was firstly synthesized and the process was given in ESI †. Then Fe_3O_4@SiO_2-MSA was synthesized according to a previous literature with a slight change.[42] Briefly, 50 mg of Fe_3O_4@SiO_2-SH nanoparticles were dispersed evenly in 30 mL of acetonitrile/water (3:1, v/v), then 5 mg of MSA and 0.5 mg of DMPA were added into it, and then the mixture was irradiated using a spectrolinker XL-1500 UV crosslinker (Spectronics Corporation, Westbury, New York) at room

Nanoscale Accepted Manuscript

temperature for 15 min. The obtained Fe_3O_4@SiO_2-MSA was washed with ethanol for 3 times, and dried under vacuum at 50 ℃ for 5 h.

Material characterization

Field emission scanning electron microscopy (FE-SEM) images were collected on a JSM-7001F scanning electron microscope and transmission electron microscopy (TEM) images were obtained by JEOL JEM-2000 EX transmission electron microscope (JEOL, Tokyo, Japan). Fourier-transform infrared (FT-IR) spectrum was conducted on Thermo Nicolet 380 spectrometer using KBr pellets (Nicolet, Wisconsin, USA). Thermogravimetrci (TG) analysis was performed under nitrogen atmosphere with a heating rate of 10 ℃ min^{-1} from room temperature to 700 ℃ (NETZSCH, Selb, Germany). The saturation magnetization curve was obtained on a Physical Property Measurement System 9T (Quantum Design, San Diego, USA) at room temperature.

Tryptic digestion of standard glycoproteins and proteins extracted from mouse liver

1 mg of human IgG, chicken avidin or HRP was respectively dissolved in 400 μL of buffer containing 100 mmol L^{-1} NH_4HCO_3 and 8 mol L^{-1} urea. After the addition of 10 μL DTT (1 mmol L^{-1}) and being kept at 60 ℃ for 1 h, the protein was alkylated by 3.7 mg IAA at room temperature in the dark for 40 min. Then the solution was diluted ten-fold with NH_4HCO_3 (50 mmol L^{-1}) and digested with trypsin (protein: enzyme = 25: 1, w/w) at 37 ℃ for 16 h. The tryptic digest was lyophilized and stored at -20 ℃ for further use.

The proteins from mouse liver were extracted by following a literature procedure, [43] and the proteins (2 mg) were dissolved in 1 mL denaturing buffer containing 50 mmol L^{-1} Tris-HCl and 8 mol L^{-1} urea. After the addition of 20 μL DTT (1 mol L^{-1}) at 60 ℃ for 1 h, the proteins were alkylated by 7.4 mg IAA at room temperature in the dark for 40 min. Then the solution was diluted ten-fold with 50 mmol L^{-1} Tris-HCl and digested with trypsin (protein: enzyme = 25: 1, w/w) at 37 ℃ for 16 h. The peptides mixture was desalted by C_{18}-SPE column, then lyophilized and kept at -20 ℃ for further use.

Selective enrichment of glycopeptides by Fe_3O_4@SiO_2@PMSA nanoparticles

The Fe_3O_4@SiO_2@PMSA nanoparticles were firstly washed and dispersed in 400 μL of loading buffer (ACN/H_2O/TFA, 86: 13.9: 0.1, v/v/v). Subsequently, 3 μg of tryptic digest of human IgG, chicken avidin, or HRP was added into it and incubated moderately at room temperature for 30 min, respectively. After that, the nanoparticles were separated from the mixed solution by applying a permanent magnet and washed with the loading buffer (400 μL) three times to remove the non-specifically adsorbed peptides, then the captured glycopeptides were eluted with the eluting buffer (ACN/H_2O/TFA, 30: 69.9: 0.1, v/v/v, 10 μL) twice and subjected to further MALDI-TOF MS analysis, or deglycosylation for LC-MS/MS analysis.

For glycopeptides enrichment from complex sample, 3 mg of Fe_3O_4@SiO_2@PMSA was incubated with tryptic digests of proteins extracted from mouse liver in 500 μL loading buffer (ACN/H_2O/TFA, 86: 13: 1, v/v/v). The mixture was incubated at room temperature for 40 min. After being washed by the loading buffer to remove the non-specifically adsorbed peptides, the captured glycopeptides were eluted with the eluting buffer (ACN/H_2O/TFA, 30: 69.9: 0.1, v/v/v, 100 μL) three times. Finally, the eluate was lyophilized and deglycosylated for LC-MS/MS analysis.

Selective enrichment of glycopeptides by HILIC-SPE tips

The fabrication of HILIC SPE tips and the enrichment procedure were carried out according to a previously described method with minor modification.[44] The detailed information was given in ESI †.

Deglycosylation of N-linked Glycopeptides by PNGase F

The captured glycopeptides in the eluate were lyophilized and then redissolved in 40 μL NH_4HCO_3 (10 mmol L^{-1}). Then, 50 units of PNGase F were added into the solution and the mixture was incubated at 37 ℃ for 12 h.

Mass spectrometry analysis

All the MALDI-TOF MS experiments were carried out in a reflector positive mode with a pulsed Nd/YAG laser at 355 nm on AB Sciex 5800 MALDI-TOF/TOF mass spectrometer (AB Sciex, CA). A 0.5 μL aliquot of the eluate and 0.5 μL of DHB matrix were successively dropped onto the MALDI plate for MS analysis. As a fine matrix, DHB was dissolved in ACN/H_2O/H_3PO_4（70: 29: 1, v/v/v, 25 mg mL^{-1}）. The mouse liver protein sample was analyzed by a Thermo Q Exactive mass spectrometer (Thermo, San Jose, CA) with a nanospray ion source and a U3000 RSLC nano-system (Thermo, San Jose, CA, USA). The deglycosylated peptides were lyophilized and redissolved in FA/H_2O (0.1: 99.9, v/v), subsequently loaded on a trap column (200 μm i.d.) packed with C_{18} AQ beads (5 μm, 120 Å, Daison, Osaka, Japan). The peptides were separated by a capillary analysis column (75 μm i.d.) packed with C_{18} AQ beads (3 μm, 120 Å, Daison, Osaka, Japan). The eluting buffer were 99.9% H_2O with 0.1% FA (buffer A) and 99.9% ACN with 0.1% FA (buffer B).The gradient elution was performed as follows: from 0 to 4 % buffer B (FA/ACN, 0.1: 99.9) for 15 min, from 4% to 45 % buffer B (FA/ACN, 0.1: 99.9) for 100 min and from 45% to 80 % buffer B (FA/ACN, 0.1: 99.9) for 5 min. After ruing with 80 % buffer B for 10 min, the separation system was equilibrated by buffer A (FA/H_2O, 0.1: 99.9, v/v) for 15 min. The MS/MS spectra were obtained in a data-independent collision induced dissociation (CID) mode, and the full mass scan was acquired from m/z 400 to 2000 with resolution of 70000. The 12 most intense ions with charge over 2 and intensity threshold higher than 104 were selected for MS/MS. The dynamic exclusion was set as 30 s.

Database searching

All the LC-MS/MS raw data were searched with MaxQuant version (1.3.0.5) against a database (uniprot.Mouse, updated on July 9th, 2014). The mass tolerances were 20 ppm for initial precursor ions and 0.5 Da for fragment ions. Two missed cleavages were allowed for trypsin restriction. The cut off false discovery rate (FDR) for all the peptides identifications including

Nanoscale Accepted Manuscript

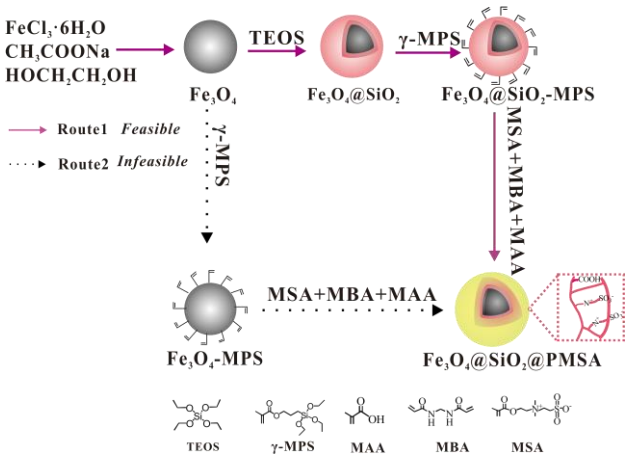

Scheme 1 Schematic illustration of the synthetic procedure for preparation of Fe_3O_4@SiO_2@PMSA nanoparticles.

the glycopeptides was controlled below 1 %. Only peptides with N-! P-S/T were considered as N-linked glycopeptides.

Results and discussion

Fabrication and characterization of Fe_3O_4@SiO_2@PMSA nanoparticles

The protocol for the synthesis of Fe_3O_4@SiO_2@PMSA nanoparticle was illustrated in **Scheme 1** (Route1). Firstly, the Fe_3O_4 nanoparticle was synthesized by a modified solvothermal reaction, and then modified with a thin layer of SiO_2 shell via a sol-gel method. Subsequently, MPS was grafted onto the Fe_3O_4@SiO_2 nanoparticle to form abundant active double bonds for the next polymerization. Finally, a robust layer of PMSA was coated on the Fe_3O_4@SiO_2-MPS core by one step reflux-precipitation polymerization with MAA as the auxiliary monomer, MSA as the zwitterionic monomer and MBA as the cross-linker to form Fe_3O_4@SiO_2@PMSA. For comparison, the Fe_3O_4@SiO_2 nanoparticle was also modified with a monolayer of MSA to obtain Fe_3O_4@SiO_2-MSA.

As it was known to all, it is hard to synthesize hydrophilic polymer coated nanoparticles by reflux-precipitation polymerization to some extend due to some hydrophilic monomers (like MSA) are insoluble in the commonly used solvent like acetonitrile. Herein, acetonitrile/water co-solvent was introduced to dissolve the monomers, cross-linker and initiator. Because of their low solubility in the co-solvent, the formed oligomers precipitated from the homogeneous solution were easily captured by the Fe_3O_4@SiO_2-MPS and the out-surface PMSA layer was obtained. To investigate the influence of the co-solvent on the following polymerization, several mixed solvent with different ratio of ACN and water (9: 1, 3: 1, 1: 1，v/v) were employed. As demonstrated in Fig. S1 (ESI†), no size increase was found when the ratios of ACN and water were 9: 1 and 1: 1. The main reason is that the mixed solvent of 90 % ACN couldn't dissolve the monomer totally so that it would prevent the following polymerization reaction. However, the co-solvent with high ratio of water was unfavourable for the reaction due to the

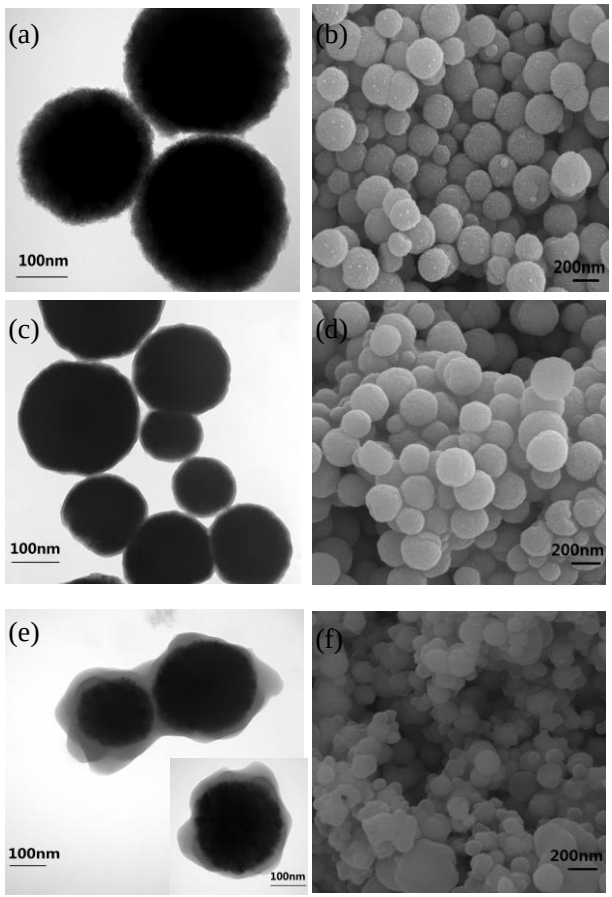

Fig.1 a) TEM and b) FESEM images of Fe_3O_4 cores. c) TEM and d) FESEM images of Fe_3O_4@SiO_2. e) TEM and f) FESEM images of Fe_3O_4@SiO_2@PMSA nanoparticles.

inner hydrogen bonding force. Besides, the addition of MAA was also a significant factor to the formation of core-shell structured nanoparticles because that the hydrogen bonding among MAA units and electrostatic bonding between MAA and MSA units make great contributions to the subsequent polymerization.

Representative TEM and FESEM images of Fe_3O_4, Fe_3O_4@SiO_2, Fe_3O_4@SiO_2@PMSA nanoparticles are shown in Fig.1. The Fe_3O_4 nanoparticles are uniform in both shape and size with an average diameter of ca. 280 nm. After coating with SiO_2, a well-defined core-shell structure appeared and the surface was smoother than Fe_3O_4 nanoparticles (Fig. 1b and Fig. 1d). The size slightly increases and the SiO_2 layer is estimated to be 10 nm in thickness (Fig. 1c). The TEM image of Fe_3O_4@SiO_2@PMSA nanoparticles (Fig. 1e) clearly indicates that the cross-linked PMSA layer has been successfully coated on the surface of Fe_3O_4@SiO_2-MPS, and the thickness of the polymer shell is around 60 nm. Furthermore, the FESEM image of Fe_3O_4@SiO_2@PMSA (Fig. 1f) with an obvious agglomeration compared to that of the Fe_3O_4@SiO_2 also reveals the successful coating of the PMSA.

Modification of Fe_3O_4 nanoparticles with SiO_2 shell is essential for the coating of the next PMSA layer. We tried to directly coat a PMSA layer onto the Fe_3O_4-MPS surface without modification

Nanoscale Accepted Manuscript

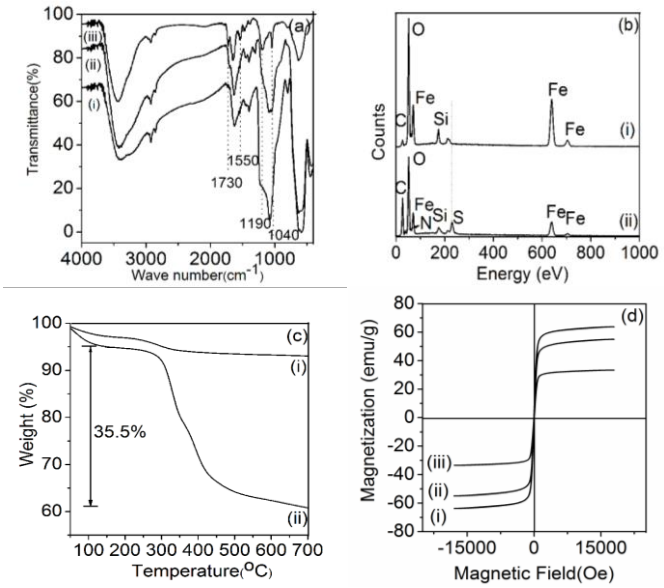

Fig. 2 (a) FT-IR spectra of (i) Fe_3O_4, (ii) Fe_3O_4@SiO_2 and (iii) Fe_3O_4@SiO_2@PMSA, (b) EDX spectrums and (c) TGA curves of (i) Fe_3O_4@SiO_2 and (ii) Fe_3O_4@SiO_2@PMSA. (d) Magnetization hysteresis loops of (i) Fe_3O_4, (ii) Fe_3O_4@SiO_2 and (iii) Fe_3O_4@SiO_2@PMSA.

(**Scheme 1**, Route 2). Unfortunately, no final core-shell structurewas obtained. We infer the primary reason is that both the Fe_3O_4 and MSA take charges in the solvent and there is a strong mutual interaction between the core and the zwitterionic monomer, subsequently seriously influencing the dispersive stability of the Fe_3O_4 nanoparticles in the solvent. The Fe_3O_4 nanoparticles subside quickly without any further reaction. Therefore, a proper interim layer is required. The interim layer should not only ensure the seed nanoparticles have a good dispersibility in the co-solvent but also give high accessibility to MSA for further polymerization reaction. Taking all these into consideration, due to its excellent hydrophilcity as well as easy modification character, the silica layer was introduced naturally to obtain the coating layer of PSMA on the magnetic cores.

FTIR spectroscopy was conducted to inspect the chemical structure of Fe_3O_4@SiO_2, Fe_3O_4@SiO_2-MPS and Fe_3O_4@SiO_2@PMSA. Compared to the FI-IR spectrum of Fe_3O_4@SiO_2 (581 cm^{-1}, $\upsilon_{Fe\text{-}O\text{-}Fe}$, 1091 cm^{-1}, $\upsilon_{Si\text{-}O\text{-}Si}$), a new characteristic adsorption peak (1730 cm^{-1}, $\upsilon_{C=O}$) in the spectrum of Fe_3O_4@SiO_2-MPS (Fig. 2a) could demonstrate the successful graft of MPS. And the new characteristic peaks appear at 1040 and 1190 cm^{-1} are ascribed to the stretching vibration of O=S=O in the $-SO_3^-$ group.[45] The peak at 1550 cm^{-1} corresponds to the bending vibration of N-H in the MBA. In addition, the adsorption peak at 1730 cm^{-1} attributed to the C=O stretching vibration is enhanced. All the evidences reveal the successful coating of PMSA on the surface of Fe_3O_4@SiO_2-MPS.

Energy dispersive X-ray (EDX) spectra and thermogravimetric analysis (TGA) were also recorded to confirm the introduction of PMSA. As shown in Fig. 2b, C, O, Si, Fe are the main elements. And the emerging of N and S elements indicates the successful modification of PMSA. TGA curve reveals that the weight loss of 6.70 % of Fe_3O_4@SiO_2 is attributed to the adsorbed water. It could be calculated that the weight loss of the Fe_3O_4@SiO_2@PMSA nanoparticles is 35.5 %, which demonstrates the high amount of PMSA on the composite nanoparticles.

The magnetic properties of three nanoparticles were studied by using a vibrating sample magnetometer at room temperature (Fig. 2d). The magnetic hysteresis loop curves show that the three kinds of materials have no obvious remanence or coercivity at room temperature, indicating that they all possess a superparamagnetic character. The superparamagnetism is coming from the small nanocrystals in the Fe_3O_4 cores, which behave as superparamagnets with a saturation magnetization (Ms) value of 64.3 emu g^{-1}. As a comparison, the Ms value of the Fe_3O_4@SiO_2 nanoparticle was 55.5 emu g^{-1}. After coating the polymer layer and the Ms value strikingly decreased to about 33.6 emu g^{-1}. The Fe_3O_4@SiO_2@PMSA nanoparticles were observed having better dispersibility and stability in water compared to Fe_3O_4@SiO_2-MSA when no external magnet field was applied. However, thanks to the high-magnetic response of Fe_3O_4 core, the final product of Fe_3O_4@SiO_2@PMSA microspheres could be separated from the solution in only 30 s by using a magnet.

Selective enrichment of glycopeptides from tryptic digest from standard glycoproteins

On the basis of hydrophilic interaction chromatography, hydrophilic materials, i.e., immobilized polysaccharides and MOFs and etc. have been reported to selectively enrich glycopeptides. [46-48] Thus, to evaluate the practicability of the Fe_3O_4@SiO_2@PMSA in the selective enrichment of glycopeptides, a tryptic digest of standard glycoprotein (human IgG) was employed as the testing sample. The workflow of glycopeptides enrichment is presented in Scheme S1a. As shown in Fig. 4a, only four glycopeptides with weak MS signal intensity and low signal-to-noise ratio (S/N) was detected for the direct analysis of IgG tryptic digest on account of the low abundance of glycopeptides and the strong signal suppression by the abundant non-glycosylated peptides. However, after being enriched by Fe_3O_4@SiO_2@PMSA nanoparticles, the signals of non-glycosylated peptides were eliminated and twenty six N-linked glycopeptides were detected and identified with high intensity and S/N ratio (Fig. 4b). For comparison, the tryptic digest of human IgG was also treated with Fe_3O_4@SiO_2-MSA, only eight glycopeptides could be detected with an inferior signal intensity and S/N ratio (Fig. 4c). The enrichment efficiency of Fe_3O_4@SiO_2@PMSA was evidently superior to that of Fe_3O_4@SiO_2-MSA, which can be ascribed to the higher surface density of zwitterionic groups on the material and stronger multivalent hydrophilic interactions. The detailed structures and the S/N ratios of the glycopeptides are listed in Tables S3 and S4 (ESI†), respectively. In addition, compared with the HILIC tips (Scheme S1b，S1c), only six glycopeptides could be noted and the intensity is relatively low (Fig. 4d) after enrichment. The enrichment performance of Fe_3O_4@SiO_2@PMSA is obviously better than that of the HILIC tips. Subsequently，on the one hand, all the enriched peptides were analyzed by MALDI-TOF MS/MS

Nanoscale Accepted Manuscript

and the spectrum of a representative glycopeptide (m/z=2763.8) with the explicite glycan structure was given in Fig. S2 (ESI†), indicating that the enriched peptides all geared to glycopeptides. On the other hand, the eluted glycopeptides were deglycosylated by PNGase F and only two deamidated peptides (m/z=1158.54, 1190.53) were detected (Fig. 4e), which further confirmed that those peaks appearing in the Fig. 4b all belonged to N-linked glycopeptides. The result indicates that Fe_3O_4@SiO_2@PMSA nanoparticles have high enrichment selec- tivity for human IgG enrichment. Superficial functional group density of the magnetic composite nanoparticles attaches great importance to the biological enrichment. In our work, a high density of zwitterionic groups on the polymerization chain is critical for achieving high performance in specific enrichment of glycopeptides.

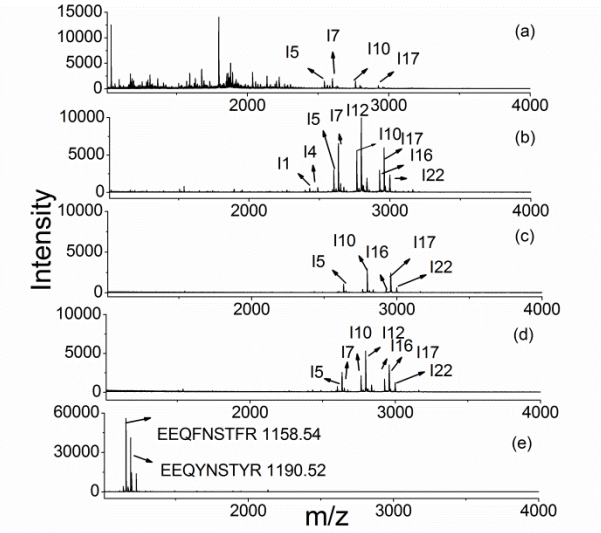

Fig.4 MALDI-TOF MS spectra of (a) direct analysis of the 0.5 pmol tryptic digest of human IgG, (b) after enrichment by Fe_3O_4@SiO_2@PMSA, (c) after enrichment by Fe_3O_4@SiO_2-MSA, (d) after enrichment by HILIC Tips and (e) deglycosylation by PNGase F.

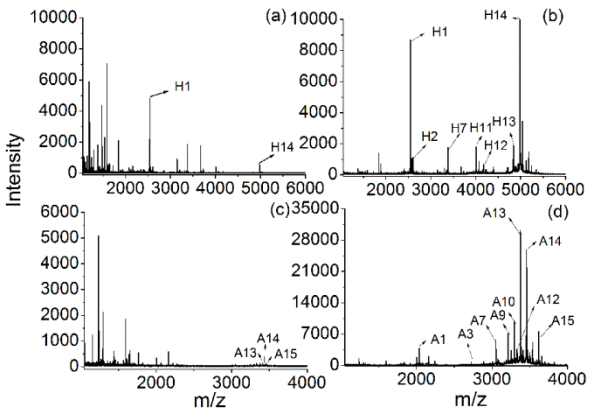

Fig. 5 MALDI-TOF MS spectra of (a) direct analysis of the 1 pmol tryptic digest of HRP, (b) after enrichment by Fe_3O_4@SiO_2@PMSA, (c) direct analysis of the 1 pmol tryptic digest of chicken avidin and (d) after enrichment by Fe_3O_4@SiO_2@PMSA.

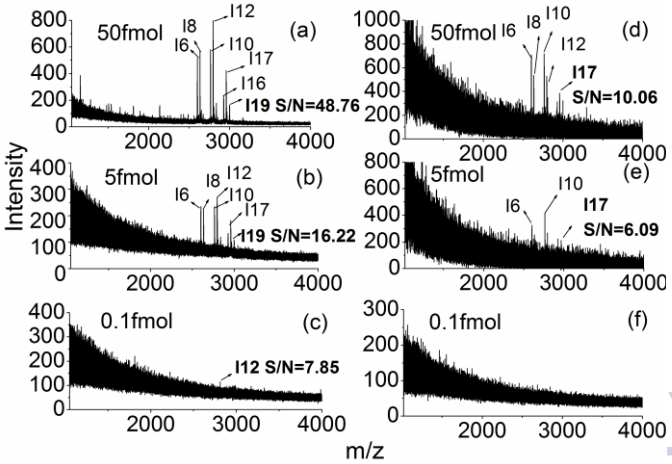

Fig.6 MALDI-TOF MS spectra of (a) 50 fmol, (b) 5 fmol and (c) 0.1 fmol human IgG digest after treatment by Fe_3O_4@SiO_2@PMSA nanoparticles; (d) 50 fmol, (e) 5 fmol and (f) 0.1 fmol human IgG digest after treatment by HILIC tips.

To further evaluate its universality for the glycopeptide enrichment, the tryptic digests of chicken avidin and HRP were also employed. A direct MALDI-TOF mass spectrum of chicken avidin is presented in Fig. 5a, and the MS signals of glycopeptides are severely suppressed by the non-glycosylated peptides. Nevertheless, fifteen glycopeptides with enhanced intensity and *S/N* ratio dominate the MS spectrum of treated sample (Fig. 5b, Table S2, ESI†). Besides, comparing to the mass spectrum of direct analysis of tryptic digest of HRP in Fig. 5c, fourteen glycopeptides (Fig. 5d, Table S1, ESI†) were identified after the enrichment by Fe_3O_4@SiO_2@PMSA. These results have revealed the high efficiency and selectivity of Fe_3O_4@SiO_2@PMSA for universal glycopeptides enrichment.

Evaluation of the detection sensitivity, binding capacity and enrichment recovery of Fe_3O_4@SiO_2@PMSA in glycopeptides enrichment

As the level of glycopeptides in a complex biological sample could be extremely low, the detection sensitivity of Fe_3O_4@SiO_2@PMSA towards glycopeptides was investigated. Tryptic IgG digest with a group of low amount of 50 fmol, 5 fmol 0.1 fmol were treated by Fe_3O_4@SiO_2@PMSA as well as the HILIC tips. As shown in Fig. 6a and Fig. 6e, several glycopeptides were clearly detected in 50 fmol of human IgG tryptic digest after enrichment by both Fe_3O_4@SiO_2@PMSA and HILIC tips. And with the amount of human IgG being decreased to 5 fmol, less glycopeptides with lower S/N ratios enriched by HILIC tips could be detected as presented in Fig. 6b and Fig. 6e. And when the total amount of human IgG was as low as 0.1 fmol, one peptide could still be detected after enrichment by Fe_3O_4@SiO_2@PMSA at S/N ratio of 7.8 with a m/z of 2795.58. However, none of glyopeptide could be identified after treatment by HILIC tips. Furthermore, the resulting detection sensitivity was also higher than previously reported HILIC materials, such as the branched PEG brushes hybrid hydrophilic magnetic

Nanoscale Accepted Manuscript

nanoparticles (0.5 fmol), zwitterionic polymer brushes hybrid silica nanoparticles

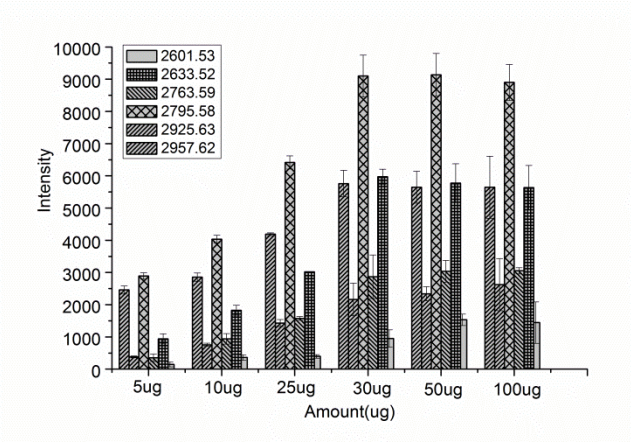

Fig.7 The intensity of six selected N-linked glycopeptides from human IgG digest after treatment with different amount of Fe_3O_4@SiO_2@PMSA nanoparticles.

Table 1 Recovery of N-linked glycopeptides from human IgG digest by using Fe_3O_4@SiO_2@PMSA

No.	m/z	Recovery ± S.D (%, n=3)
I6	2601.53	73.6±2.8
I8	2633.52	94.8±1.5
I10	2763.59	93.9±1.7
I12	2795.58	101.2±0.7
I16	2925.63	106.2±0.8
I17	2957.62	109.3±1.1

(10 fmol) and silica-based click maltose (30 fmol). [23, 44, 45] The lower detection limit may be attributed to the excellent hydrophilicity, absolute magnetic separation, a large amount of MSA groups as well as stronger multivalent hydrophilic interactions. This result shows that the prepared Fe_3O_4@SiO_2@PMSA nanoparticle significantly improves detection sensitivity for glycopeptides.

To inspect the binding capacity of Fe_3O_4@SiO_2@PMSA, different amounts of Fe_3O_4@SiO_2@PMSA (5-100 μg) were added to a fixed amount of human IgG digest (3 μg). After the enrichment, the eluted fraction was analyzed by MALDI-TOF MS. The signal intensities of six selected glycopeptides reached the maximum when the addition of the nanoparticles was 30 μg and the binding capacity was calculated to be 100 mg g^{-1} (Fig. 7). The large binding capacity might be owing to the high amount of zwitterionic groups and the strong multivalent hydrophilic interactions between the glycopeptides and the material.

Stable-isotope dimethyl labeling method [49] was utilized for evaluating the recovery yield of Fe_3O_4@SiO_2@PMSA for glycopeptides enrichment. Briefly, equal amount of human IgG (3 μg) tryptic digest was labelled with light and heavy isotopes, respectively. The heavy-tagged digest was enriched with Fe_3O_4@SiO_2@PMSA abiding by the above-mentioned enrichment procedure. The resulting eluent was mixed and the mixture was re-enriched by Fe_3O_4@SiO_2@PMSA, then the eluent was analyzed by MALDI-TOF MS. The recovery was calculated by the signal intensity ratio of heavy isotope-labelled glycol-peptides divided by the light isotope-labelled glycopeptides. The recovery yields of six selected peptides were all over 73.6 % (Table 1.) The result reveals that the Fe_3O_4@SiO_2@PMSA nanoparticle is an ideal affinity material for the enrichment of glycopeptides.

Application in glycopeptide enrichment from real complex biological sample

Inspired by the outstanding enrichment efficiency in standard glycoprotein tryptic digest, the Fe_3O_4@SiO_2@PMSA nanoparticles were further applied to the analysis of glycoproteome of mouse liver. 65 μg of proteins extracted from mouse liver were incubated with Fe_3O_4@SiO_2@PMSA as well as the HILIC tips, and the eluent was loyophilized, deglycosylated and analyzed by nano LC-MS/MS, followed by database searching with controlling the false discovery rate (FDR) for all the peptides identifications including the glycopeptides < 1%. As a result, a total of 905 N-glycosylation sites from 458 N-glycoproteins were identified with a consensus sequence of N-! P-S/T motif (Table S5, ESI†).The explicite data of three independent runs are shown in Fig. S3(ESI†). In comparison, only 457 N-glycosylation sites from 269 N-glycoproteins were identified by HILIC tips. The differences in the structure of these materials contributed to the different performance of glycopeptide enrichment. The result clearly demonstrates that the Fe_3O_4@SiO_2@PMSA nanoparticles own high selectivity and effectiveness characters in the enrichment of low-abundant N-linked glycopeptides from complex biological samples.

Conclusions

In summary, a facile, repeatable, and robust synthetic route for preparation of a new HILIC material, Fe_3O_4@SiO_2@PMSA nanoparticle, with well-defined core-shell structure was presented. The characterization results showed that the SiO_2 interim layer and the ratio of the co-solvent had strong effects on the successful preparation. The thick polymer layer improved the hydrophilicity and the amount of zwitterionic molecules on the polymerization chains. The glycopeptides enrichment experiments confirmed that the Fe_3O_4@SiO_2@PMSA nanoparticles have high specificity, extremely high detection sensitivity, large binding capacity and satisfactory recovery. In the selective enrichment of N-linked glycopeptides from tryptic digest of proteins extracted from mouse liver, the Fe_3O_4@SiO_2@PMSA shows great practicability in identifying low-abundant glycopeptides from minute amounts of complex biological samples. It can be expected that the as-synthesized Fe_3O_4@SiO_2@PMSA would hold great potential in glycoproteome research.

Acknowledgements

Financial support is gratefully acknowledged from the National Natural Sciences Foundation of China (21235006), the National Natural Science Foundation of China (No.21475044), the Science

Nanoscale Accepted Manuscript

and Technology Commission of Shanghai Municipality (12JG0500200), the Creative Research Group Project by NSFC (2132106), the National Key Scientific Instrument and Equipment Development Project (2012YQ120044), the China State Key Basic Research Program Grant (2013CB911202, 2012CB-910601 and 2012CB-910101), the Analytical Method Innovation Program of MOST (2012M030900), and the Knowledge Innovationprogram of DICP to H.F.Z.

[a]*Shanghai Key Laboratory of Functional Materials Chemistry, East China University of Science and Technology, Shanghai 200237, China. E-mail: weibingzhang@ecust.edu.cn*
[b]*CAS Key Laboratory of Separation Sciences for Analytical Chemistry, National Chromatographic R&A Center, Dalian Institute of Chemical Physics, Chinese Academy of Sciences (CAS), Dalian 116023, China. E-mail: hanfazou@dicp.ac.cn*

Yajing Chen and Zhichao Xiong contributed equally to this work.

Notes and references

1. A. Helenius and M. Aebi, *Science*, 2001, **291**, 2364-2369.
2. K. Ohtsubo and J. D. Marth, *Cell*, 2006, **126**, 855-867.
3. J. W. Dennis, I. R. Nabi and M. Demetriou, *Cell*, 2009, **139**, 1229-1241.
4. G. W. Hart and R. J. Copeland, *Cell*, 2010, **143**, 672-676.
5. J. A. Ludwig and J. N. Weinstein, *Nat. Rev.Cancer*, 2005, **5**, 845-856.
6. S. Feng, N. Yang, S. Pennathur, S. Goodison and D. M. Lubman, *Ana.Chem.*, 2009, **81**, 3776-3783.
7. Z. Zeng, M. Hincapie, S. J. Pitteri, S. Hanash, J. Schakwijk, J. M. Hogan, H. Wang and W. S. Hancock, *Ana. Chem.*, 2011, **83**, 4845-4854.
8. H. Kaji, H. Saito, Y. Yamauchi, T. Shinkawa, M. Taoka, J. Hirabayashi, K. Kasai, N. Takahashi and T. Isobe, *Nat. Biotechnol.* , 2003, **21**, 667-672.
9. L. Li, Y. Lu, Z. J. Bie, H. Y. Chen and Z. Liu, *Angew. Chem., Int. Ed.*, 2013, **52**, 7451-7454.
10. Y. C. Liu, L. B. Ren and Z. Liu, *Chem. Commun.*, 2011, **47**, 5067-5069.
11. Y. C. Liu, Y. Lu and Z. Liu, *Chem. Sci.*, 2012, **3**, 1467-1471.
12. Z. Bie, Y. Chen, H. Li, R. Wu and Z. Liu, *Anal. Chim. Acta.*, 2014, **834**, 1-8.
13. H. Li, H. Wang, Y. Liu and Z. Liu, *Chem. Commun.*, 2012, **48**, 4115-4117.
14. Z. Sun, J. Q. Dong, S. Zhang, Z. Y. Hu, K. Cheng, K. Li, B. Xu, M. L. Ye, Y. Z. Nie, D. M. Fan and H. F. Zou, *J. Proteome Res.*, 2014, **13**, 1593-1601.
15. J. Zhu, Z. Sun, K. Cheng, R. Chen, M. L. Ye, B. Xu, D. G. Sun, L. M. Wang, J. Liu, F. J. Wang and H. F. Zou, *J. Proteome Res.*, 2014, **13**, 1713-1721.
16. J. Zhu, F. J. Wang, K. Cheng, J. Dong, D. G. Sun, R. Chen, L. M. Wang, M. L. Ye and H. F. Zou, *Proteomics*, 2013, **13**, 1306-1313.
17. L. Cao, L. Yu, Z. Guo, A. Shen, Y. Guo and X. Liang, *J. Proteome Res.*, 2014, **13**, 1485-1493.
18. Y. Takegawa, K. Deguchi, H. Ito, T. Keira, H. Nakagawa and S. I. Nishimura, *J. Sep. Sci.*, 2006, **29**, 2533-2540.
19. Y. Wada, M. Tajiri and S. Yoshida, *Anal. Chem.*, 2004, **76**, 6560-6565.
20. A. J. Shen, Z. M. Guo, L. Yu, L. W. Cao and X. M. Liang, *Chem. Commun.*, 2011, **47**, 4550-4552.
21. Z. C. Xiong, Y. S. Ji, C. L. Fang, Q. Q. Zhang, L. Y. Zhang, M. L. Ye, W. B. Zhang and H. F. Zou, *Chem.-Eur. J.*, 2014, **20**, 7389-7395.
22. H. Huang, Y. Jin, M. Xue, L. Yu, Q. Fu, Y. Ke, C. Chu and X. Liang, *Chem. Commun.*, 2009, 6973-6975.
23. Z. C. Xiong, L. Zhao, F. J. Wang, J. Zhu, H. Q. Qin, R. A. Wu, W. B. Zhang and H. F. Zou, *Chem. Commun.*, 2012, **48**, 8138-8140.
24. N. A. Frey, S. Peng, K. Cheng and S. H. Sun, *Chem. Soc. Rev.*, 2009, **38**, 2532-2542.
25. A. H. Lu, E. L. Salabas and F. Schuth, *Angew. Chem., Int. Ed.*, 2007, **46**, 1222-1244.
26. H. H. P. Yiu, H. J. Niu, E. Biermans, G. van Tendeloo and M. J. Rosseinsky, *Adv. Funct. Mater.*, 2010, **20**, 1599-1609.
27. Y. Chen, H. R. Chen, S. J. Zhang, F. Chen, L. X. Zhang, J. M. Zhang, M. Zhu, H. X. Wu, L. M. Guo, J. W. Feng and J. L. Shi, *Adv. Funct. Mater.*, 2011, **21**, 270-278.
28. X. J. Wang, N. Xia and L. Liu, *Int. J. Mol. Sci.*, 2013, **14**, 20890-20912.
29. C. H. Yeh, S. H. Chen, D. T. Li, H. P. Lin, H. J. Huang, C. I. Chang, W. L. Shih, C. L. Chern, F. K. Shi and J. L. Hsu, *J. Chromatogr. A*, 2012, **1224**, 70-78.
30. Z. C. Xiong, H. Q. Qin, H. Wan, G. Huang, Z. Zhang, J. Dong, L. Y. Zhang, W. B. Zhang and H. F. Zou, *Chem. Commun.*, 2013, **49**, 9284-9286.
31. C. L. Fang, Z. C. Xiong, H. Q. Qin, G. Huang, J. Liu, M. L. Ye, S. Feng and H. F. Zou, *Anal. Chim. Acta*, 2014, **841**, 99-105.
32. S. Y. Jiang and Z. Q. Cao, *Adv. Mater.*, 2010, **22**, 920-932.
33. J. Wu, W. F. Lin, Z. Wang, S. F. Chen and Y. Chang, *Langmuir*, 2012, **28**, 7436-7441.
34. Y. He, J. Hower, S. F. Chen, M. T. Bernards, Y. Chang and S. Y. Jiang, *Langmuir*, 2008, **24**, 10358-10364.
35. S. F. Chen, J. Zheng, L. Y. Li and S. Y. Jiang, *J. Am. Chem. Soc.*, 2005, **127**, 14473-14478.
36. M. Wuhrer, A. R. de Boer and A. M. Deelder, *Mass Spectrom. Rev.*, 2009, **28**, 192-206.
37. P. J. Boersema, S. Mohammed and A. J. R. Heck, *Anal. Bioanal. Chem.*, 2008, **391**, 151-159.
38. L. Mauko, A. Nordborg, J. P. Hutchinson, N. A. Lacher, E. F. Hilder and P. R. Haddad, *Anal. Biochem.*, 2011, **408**, 235-241.
39. X. Q. Xu, C. H. Deng, M. X. Gao, W. J. Yu, P. Y. Yang and X. M. Zhang, *Adv. Mater.*, 2006, **18**, 3289-+.
40. J. P. Ge, Q. Zhang, T. R. Zhang and Y. D. Yin, *Angew. Chem., Int. Ed.*, 2008, **47**, 8924-8928.
41. G. W. He, Z. Y. Li, Y. F. Li, Z. Li, H. Wu, X. L. Yang and Z. Y. Jiang, *Acs Appl. Mater. Inter.*, 2014, **6**, 5362-5366.
42. M. Fiore, A. Marra and A. Dondoni, *J. Org. Chem.*, 2009, **74**, 4422-4425.
43. M. M. Dong, M. L. Ye, K. Cheng, C. X. Song, Y. B. Pan, C. L. Wang, Y. Y. Bian and H. F. Zou, *J. Proteome Res.*, 2012, **11**, 4673-4681.

Nanoscale Accepted Manuscript

44. J. Zhu, F. J. Wang, R. Chen, K. Cheng, B. Xu, Z. M. Guo, X. M. Liang, M. L. Ye and H. F. Zou, *Anal. Chem.*, 2012, **84**, 5146-5153.
45. G. Huang, Z. C. Xiong, H. Q. Qin, J. Zhu, Z. Sun, Y. Zhang, X. J. Peng, J. J. Ou and H. F. Zou, *Anal. Chim. Acta*, 2014, **809**, 61-68.
46. L. Yu, X. L. Li, Z. M. Guo, X. L. Zhang and X. M. Liang, *Chem.-Eur. J.*, 2009, **15**, 12618-12626.
47. Y.-W. Zhang, Z. Li, Q. Zhao, Y.-L. Zhou, H.-W. Liu and X.-X. Zhang, *Chem. Commun.*, 2014, **50**, 11504-11506.
48. Y. Ji, Z. Xiong, G. Huang, J. Liu, Z. Zhang, Z. Liu, J. Ou, M. Ye and H. Zou, *Analyst*, 2014, **139**, 4987-4993.
49. P. J. Boersema, R. Raijmakers, S. Lemeer, S. Mohammed and A. J. R. Heck, *Nat. Protoc.*, 2009, **4**, 484-494.

Nanoscale Accepted Manuscript